Electron Transition Current Density in Molecules. 3. *Ab Initio* Calculations for Vibrational Transitions in Ethylene and Formaldehyde

Teresa B. Freedman,* Mei-Ling Shih, Eunah Lee, and Laurence A. Nafie*

Contribution from the Department of Chemistry and W. M. Keck Center for Molecular Electronics, Syracuse University, Syracuse, New York 13244-4100

Received January 17, 1997. Revised Manuscript Received July 16, 1997[⊗]

Abstract: We present the first examples of *ab initio* calculations of electron transition current density (TCD) for vibrational transitions in molecules. The non-Born−Oppenheimer (non-BO) theoretical expressions for TCD, derived in the first paper in this series, are implemented at the *ab initio* level for the 6 vibrational transitions of formaldehyde and the 12 vibrational transitions of ethylene. Vector field calculations of the TCD were carried out with 6-31G(d) and larger basis sets and displayed with the AVS visualization software program package. TCDs for vibrational transitions arise from the non-BO correlation of electron current density to nuclear velocities. The formalism used to express this correlation is the complete adiabatic approximation in which the electronic wave function carries an explicit dependence on the nuclear velocities as well as the usual dependence on positions. Vibrational TCDs provide a unique, unambiguous visualization of electronic motion in molecules that accompanies the vibrational nuclear motion. Patterns of calculated TCD in formaldehyde and ethylene are analyzed in terms of their group theoretical properties and allowed multipole transitions. Two principal classes of TCD motion are observed. One is motion that reflects linear, laminar current densities that lead to changes in electron probability density in response to nuclear displacements. A second is circulatory motion of TCD about atomic centers that appears be associated primarily with the lateral motion of two adjacent atomic centers. The latter motion does not lead to changes in electron probability density, but gives rise to magnetic dipole moments, and is likely important in the generation of vibrational circular dichroism intensity.

Introduction

Depiction and animation of calculated nuclear displacement vectors for normal modes of vibration is a powerful visual method for understanding the nuclear contribution to molecular vibrations. However, the flow of electron density resulting from nuclear vibrational motion is only partially and indirectly known through the numerical values of atomic polar tensors. Recent theoretical development and implementation of calculations of electronic transition current density (TCD) in papers 1[1] and 2[2] of this series have now provided a method for directly visualizing electronic current during vibrational excitation. Transition current density maps, which are shown to be closely related to plots of the integrand of the molecular orbital expression for the velocity-form electric dipole transition moment, provide a vector field representation of the motion of electron density at each point in space, resulting from a transition-inducing perturbation. We present here the first calculations of vibrational transition current density for the normal modes of ethylene and formaldehyde. This *ab initio* implementation for calculating vibrational TCD vector fields and presentation of TCD maps for vibrations yield electronic current density patterns for electron flow, induced by the nuclear motion, that involve charge circulation about atomic centers, as well as electronic motion that generally follows the nuclear displacement.

Theoretical Formalism

In paper 1[1] of this series, the transition current density for a general transition between vibrational levels ν and ν' in electronic state e was defined as a sum over excited electronic states

$$J_{e\nu,e\nu'}(r) = 2\sum_{A,\alpha}\left[\sum_{s\neq e}\frac{D^0_{se,A\alpha}J^0_{es}(r)}{\omega^0_{se}}\right]\langle\phi_{e\nu}|i\dot{R}_{A\alpha}|\phi_{e\nu'}\rangle \quad (1)$$

where

$$J^0_{es}(r) = (\hbar/2m)[\Psi^0_e\nabla\Psi^0_s - \Psi^0_s\nabla\Psi^0_e] \quad (2)$$

is the electron transition current density for the e → s electronic transition with radial frequency ω^0_{se}

$$D^0_{se,A\alpha} = \langle\Psi^0_s|(\partial\Psi_e/\partial R_{A\alpha})_0\rangle \quad (3)$$

and $\dot{R}_{A\alpha}$ represents a component of the velocity vector for nucleus A at position R_A.

For a fundamental vibrational transition for mode a in the ground electronic state g, the vibrational transition current density becomes

$$J^a_{g0,g1}(r) = 2\sum_{A,\alpha}\left[\sum_{s\neq g}\frac{\left\langle\Psi^0_s\left|\left(\frac{\partial\Psi_g}{\partial R_{A\alpha}}\right)_0\right\rangle J^0_{gs}(r)\right.}{\omega^0_{sg}}\right]\langle\phi^a_{g0}|i\dot{R}_{A\alpha}|\phi^a_{g1}\rangle \quad (4)$$

These expressions for vibrational TCD make use of the complete adiabatic approximation,[3,4] which includes the non-Born−Oppenheimer correlation between electronic and nuclear velocities via the explicit parametric dependence of electronic

[⊗] Abstract published in *Advance ACS Abstracts,* September 15, 1997.

(1) Nafie, L. A. *J. Phys. Chem.*, in press.

(2) Freedman, T. B.; Gao, X.; Shih, M.-L.; Nafie, L. A. *J. Phys. Chem.*, submitted.

(3) Nafie, L. A. *J. Chem. Phys.* **1983**, *79*, 4950−4957.

(4) Nafie, L. A. *J. Chem. Phys.* **1992**, *96*, 5687−5702.

S0002-7863(97)00156-X CCC: $14.00

wave functions on nuclear velocity. The integrated form of $J^{a}_{g0,g1}(r)$ is the electronic contribution to the velocity-form electric dipole transition moment for mode a.

By expanding the nuclear velocity in the normal mode conjugate momenta $P_{a'}$,

$$J^{a}_{g0,g1}(r) = 2i\sum_{A,\alpha}\left[\sum_{s\neq g}\frac{\left\langle \Psi^{0}_{s}\left|\left(\frac{\partial \Psi_{g}}{\partial R_{A\alpha}}\right)_{0}\right\rangle J^{0}_{gs}(r)}{\omega^{0}_{sg}}\right]\left\langle \phi^{a}_{g0}\left|\sum_{a'}\left(\frac{\partial \dot{R}_{A\alpha}}{\partial P_{a'}}\right)_{0}P_{a'}\right|\phi^{a}_{g1}\right\rangle \quad (5)$$

substituting the position form nuclear displacement vectors

$$\left(\frac{\partial R_{A\alpha}}{\partial Q_{a}}\right)_{0} = \left(\frac{\partial \dot{R}_{A\alpha}}{\partial P_{a}}\right)_{0} \quad (6)$$

and rearranging, we obtain the vibrational TCD in terms of normal coordinates Q_a,

$$J^{a}_{g0,g1}(r) = 2i\sum_{s\neq g}\left[\frac{\left\langle \Psi^{0}_{s}\left|\left(\frac{\partial \Psi_{g}}{\partial Q_{a}}\right)_{0}\right\rangle J^{0}_{gs}(r)}{\omega^{0}_{sg}}\right]\langle \phi^{a}_{g0}|P_{a}|\phi^{a}_{g1}\rangle \quad (7a)$$

$$= 2i\sum_{e\neq g}\frac{D^{0}_{sg,a}J^{0}_{gs}(r)}{\omega^{0}_{sg}}\langle \phi^{a}_{g0}|P_{a}|\phi^{a}_{g1}\rangle \quad (7b)$$

Pure vibrational transition probability density (TPD) is defined from paper 1[1] in the present notation as

$$\Theta^{a}_{g0,g1}(r) = 2\sum_{s\neq e}D^{0}_{sg,a}\Theta^{0}_{gs}(r)\langle \phi^{a}_{g0}|Q_{a}|\phi^{a}_{g1}\rangle \quad (8)$$

where

$$\Theta^{0}_{gs}(r) = \Psi^{0}_{g}(r)\Psi^{0}_{s}(r) \quad (9)$$

is the pure electronic TPD for the g → s electronic transition. The vibrational TPD depends on nuclear position and not on nuclear velocity and thus lies within the Born−Oppenheimer approximation. The vector field $r\Theta^{a}_{g0,g1}(r)$ is the integrand of the electronic contribution to the position-form electric dipole transition moment for the fundamental vibrational transition for mode a. Although both position and velocity forms of the electric dipole transition moment are origin independent, the integrand $r\Theta^{a}_{g0,g1}(r)$ does depend on the choice of origin and thus does not define a unique vector field, whereas the vibrational TCD in eq 5 or 7 is uniquely defined at each point in space.

Implementation of Theory

The calculation of vibrational transition current density from eq 7 has been implemented as a sum-over-states calculation employing the single electron transition approximation (STA) for each ground-to-excited state pair in the sum. With the STA approximation, transitions in the sum-over-states involve all possible excitations of a single electron from an occupied to an unoccupied molecular orbital. This approximation has proved tenable in sum-over-states calculations implemented for vibrational circular dichroism (VCD) intensities, which have yielded reasonable values for the velocity-form electric dipole transition moment and the magnetic dipole transition moment for vibrational modes, and VCD intensities in very good agreement with experiment. We note that, in general, calculations of the non-Born−Oppenheimer velocity form of the electric dipole transition moment, whether by sum-over-states or vector-field perturbation approaches, yield values in poorer agreement with experimental vibrational intensities than do calculations of the position form electric dipole transition moment, a ground state, Born−Oppenheimer property.[5−7]

The electron transition current density terms, $J^{0}_{gs}(r)$, in eq 7, are calculated over a grid of points as described for single electronic excitations in paper 2 in this series,[2] by employing a modification of Link 604 of Gaussian 92.[8] For each vibration, each of these $J^{0}_{gs}(r)$ grid terms is multiplied by the corresponding vibronic coupling term $D^{0}_{sg,a}$, and then these products for all possible single excitations are summed. Code for calculating $D^{0}_{sg,a}$ was adapted from that for sum-over-states vibronic coupling calculations of VCD intensity developed at the University of Calgary (program VCT90)[5] and Syracuse University (program VCT94). For the *ab initio* calculations, the optimized geometries and vibrational frequencies and displacements were calculated with Gaussian 92[8] or Gaussian 94,[9] with a 6-31G(d) basis set for formaldehyde and both 6-31G(d) and 6-311-(2+,2+)G(p,d)[10] basis sets for ethylene. The Gaussian 92 or 94 read−write files from the frequency calculation were employed to obtain required atomic and molecular orbital parameters and nuclear positions and displacements in the subsequent calculation of TCD. For these small symmetrical molecules, the normalized nuclear displacement vectors were found to be identical for corresponding normal modes calculated with SCF (Hartree-Fock) and density functional theory [Becke 3-Lee-Yang-Parr (DFT/Becke3LYP) functional] methods.

Visualization of the vibrational transition current density vector field was achieved by employing the AVS visualization software (Advanced Visualization Systems, Waltham, MA) for plotting two-dimensional projections of the TCD vectors superimposed on projected wire-frame models of the molecular structure and projected nuclear displacement vectors, both of the latter obtained by use of the AVS Chemistry Viewer (Molecular Simulations, Inc., Burlington, MA). The AVS networks designed for the visualization of vibrational TCD are similar to those designed for electronic TCD described in paper 2 in this series,[2] with the addition of projections of the nuclear displacement vectors. In addition, for vibrational transitions, we have provided options to delete contour intervals and remove color maps to simplify the presentations.

We find that electronic transitions in the sum-over-states calculation involving large contributions from nonvalence 1s orbitals on heavy atoms in some cases produce very large TCD

(5) Yang, D.; Rauk, A. *J. Chem. Phys.* **1992**, *97*, 6517−6534.
(6) Freedman, T. B.; Nafie, L. A. *Chem. Phys. Lett.* **1986**, *126*, 441−446.
(7) Amos, R. D.; Jalkanen, L. J.; Stephens, P. J. *J. Phys. Chem.* **1988**, *92*, 5571−5575.
(8) Frisch, M. J.; Trucks, G. W.; Head-Gordon, M.; Gill, P. M. W.; Wong, M. W.; Foresman, J. B.; Johnson, B. G.; Schlegel, H. B.; Robb, M. A.; Replogle, E. S.; Gomperts, R.; Andres, J. L.; Raghavachari, K.; Binkley, J., S.; Gonzalez, C.; Martin, R. L.; Fox, D. J.; Defrees, D. J.; Baker, J.; Stewart, J. J. P.; Pople, J. A. *Gaussian 92, Revision C*; Gaussian, Inc.: Pittsburgh, PA, 1992.
(9) Frisch, M. J.; Trucks, G. W.; Schlegel, H. B.; Gill, P. M. W.; Johnson, B. G.; Robb, M. A.; Cheeseman, J. R.; Keith, T.; Petersson, G. A.; Montgomery, J. A.; Raghavachari, K.; Al-Laham, M. A.; Zakrzewski, V. G.; Ortiz, J. V.; Foresman, J. B.; Peng, C. Y.; Ayala, P. Y.; Chen, W.; Wong, M. W.; Andres, J. L.; Replogle, E. S.; Gomperts, R.; Martin, R. L.; Fox, D. J.; Binkley, J. S.; Defrees, D. J.; Baker, J.; Stewart, J. P.; Head-Gordon, M.; Gonzalez, C.; Pople, J. A. *Gaussian 94*, B.3 ed.; Gaussian, Inc.: Pittsburgh, PA, 1995.
(10) Wiberg, K. B.; Hadad, C. M.; Foresman, J. B.; Chupka, W. A. *J. Phys. Chem.* **1992**, *96*, 10756−10768.

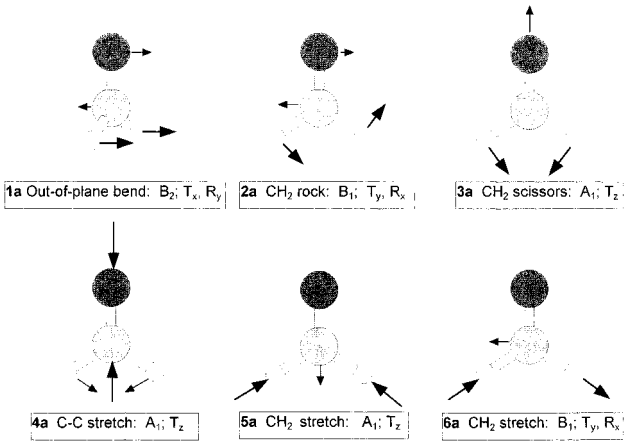

Figure 1. Description, symmetry species, and translational (T_α) and/or rotational (R_α) character of the six normal modes of formaldehyde. Arrows reflect the calculated relative nuclear displacements but are not necessarily to scale.

arrows at the nuclear positions, which perfectly follow the nuclear motion and tend to swamp the effects of valence electrons. In order to amplify the TCD due to valence electrons, we have included an option to ignore the contributions from such inner shell transitions (i.e., transitions from the *n* lowest energy to the *n* highest energy molecular orbitals, where *n* is the number of heavy atoms), equivalent to allowing some of the 1s electron density to shield the nucleus and effectively reduce the nuclear charge responsible for the nuclear contribution to the electric dipole transition moment. We also note that, in the TCD plots for vibrational modes, we have depicted the (positive) electron current displacement, not the charge displacement, which results in a clearer view of the direct effect of the nuclear velocities on the electron current. In the calculation of the electric dipole transition moment, the integration over all the TCD current vectors, the opposite charges for the electronic and nuclear contributions is of course taken into account.

Results

The descriptions, symmetry species, and translational (T_α, $\alpha = x, y,$ or z) or rotational (R_α) character of the six normal modes of formaldehyde are shown in Figure 1. The corresponding vibrational TCD maps for these six vibrations are presented in Figure 2, along with wire-frame models of the molecule and the relative nuclear displacement vectors ($\partial R_{A\alpha}/\partial Q_a$). These calculations were obtained at the HF/6-31g(d) level by ignoring the contributions from the inner shell 1s orbitals on carbon and oxygen, as described above, to more clearly view the contributions from valence orbitals. The color maps in Figure 2 reveal the regions of largest transition current density. For the totally symmetric modes 3a, 4a, and 5a, the TCD generally follows the nuclear motion, with the largest TCD observed for nuclear displacement along the bond direction. In mode 4a, the TCD

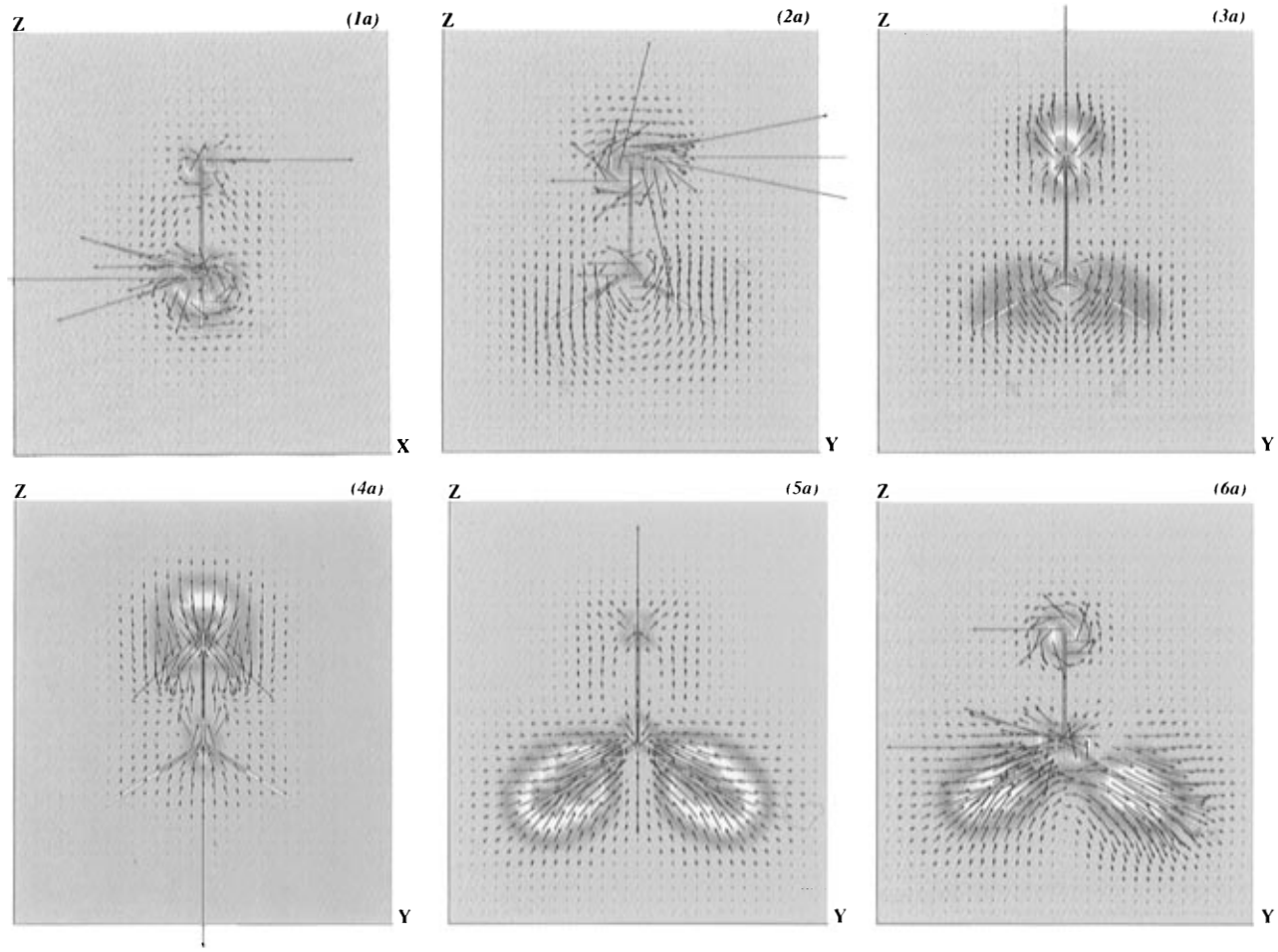

Figure 2. 2D projections of vibrational transition current density vectors (black arrows) and nuclear displacement vectors (orange arrows) for the six normal modes of formaldehyde, superimposed on wire-frame projections of the molecular structure. Color map [blue (smallest) → red (largest)] denotes the magnitudes of the TCD vectors in that region. Mode numbers correspond to the descriptions and assignments in Figure 1. Projection plane for the current for the out-of-plane bend (mode 1a) is perpendicular to the plane of the molecule through the C═O bond. Projection plane for the in-plane modes is the plane of the molecule. Nuclear displacement vectors have been scaled for clarity for the set of vibrations; TCD vectors are scaled the same for all six modes.

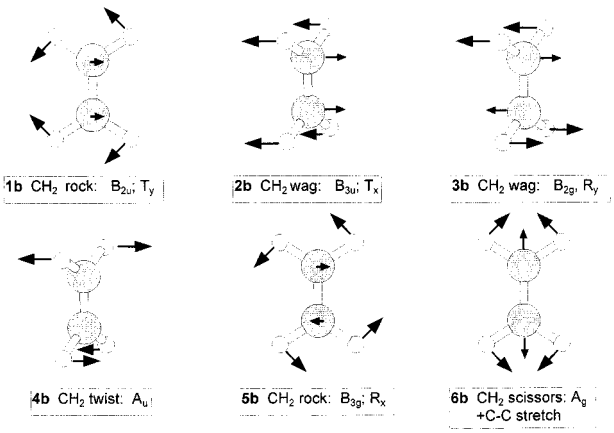

Figure 3. Description, symmetry species, and translational and/or rotational character of the six lowest frequency normal modes of ethylene.

that is generally transverse to the CH bonds arising from the CH_2 scissoring contribution (seen clearly for mode 3a) is canceled by the larger opposing TCD from the C═O bond contraction displacement of the carbon nucleus. The nuclear-following TCD contributes to the electric dipole transition moment for the mode and integrates to net electron displacement in the z-direction, as required for A_1 symmetry. This type of vibrational TCD leads to changes in the electron probability density and resembles laminar current flow. In the nontotally symmetric modes 1a, 2a, and 6a, in addition to nuclear following TCD (net *y*-displacement for B_1 modes 2a and 6a, and net *x*-displacement for B_2 mode 1a), local circulatory current density about the oxygen and carbon nuclei is observed. Such motion appears to accompany the opposing lateral motion of adjacent nuclei. This motion, along with the angular current flow along the H−C−H bonds in mode 6a, contributes to the magnetic dipole transition moment (R_x or R_y character) for the vibrational transition.

The 12 normal modes of ethylene are described in Figures 3 and 5, with the corresponding vibrational TCD maps (6-31G-(d) basis, ignoring 1s transitions) presented in Figures 4 and 6. Additional 2D slices of the TCD for the CH_2 twisting mode 4b of ethylene are shown in Figure 7. Similar to the formaldehyde TCD maps, the symmetry and electric dipole or magnetic dipole-allowed characters are clearly revealed for each mode. The bond stretching motions (modes 6b, 8b, 9b, 10b, 11b, and 12b) produce electron transition current density that generally follows the nuclear motion along the bond direction, and in-plane deformation motions (rocks 1b and 5b; scissors 6b and 7b) generate vibrational TCD generally transverse to the bond. In the C−C stretching mode 8b, the TCD from the bond stretch dominates that from the CH_2 scissoring contribution. For the two in-plane CH_2 rocks (1b and 5b), the rocking motion at each methylene group produces a local circulation of electronic charge encompassing the entire group. As required by symmetry, the net sense of circulation is opposite for the two groups for the B_{2u} mode (1b), for which the circulatory motion cancels and the linear charge motion sums to net flow in the *y* direction, whereas in the B_{2g} mode (5b), the net translational TCD is zero, but there is net charge circulation (R_x character) about the entire

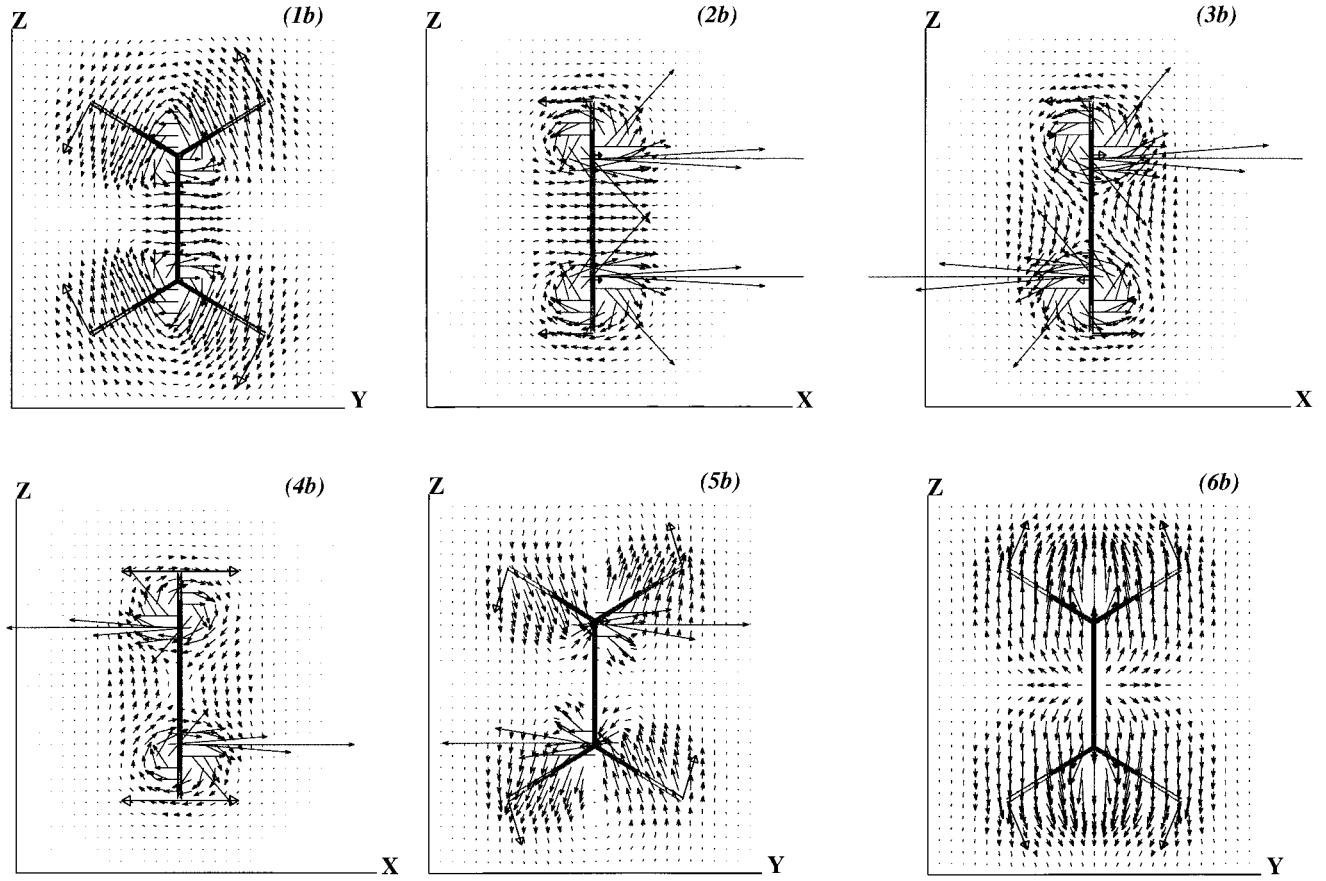

Figure 4. 2D projections of vibrational transition current density (small arrows) and nuclear displacements (large arrows) for the six normal modes of ethylene described in Figure 3, superimposed on wire-frame projections of the molecular structure. The color background has been removed for simplicity of presentation. Projection plane for the current and displacements for the out-of-plane modes (2b, 3b, 4b) is perpendicular to the plane of the molecule through the C═C bond. Projection plane for the in-plane modes (1b, 5b, 6b) is the plane of the molecule. Nuclear displacement arrows have been scaled for clarity for the set of ethylene vibrations. TCD vectors have been scaled up by a factor of 5×10^6 for mode 4b, compared to those for the remaining modes shown in Figures 4, 6, and 7.

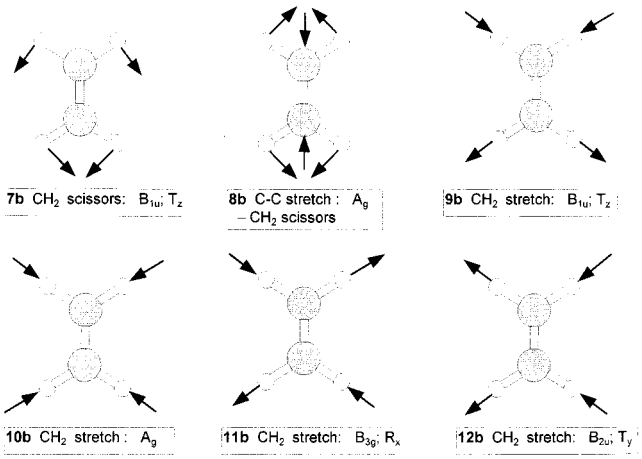

Figure 5. Description, symmetry species, and translational and/or rotational character of the six highest frequency normal modes of ethylene.

molecule. Neither the nuclear nor the electronic motion produces local charge circulation in the scissoring modes (6b and 7b). The antisymmetric CH_2 stretches 11b and 12b also involve local charge circulation within each methylene group that cancels for the B_{2u} mode (12b) and reinforces for the B_{3g} mode (11b).

For the A_u twisting mode 4b, the net TCD in the plane through the C═C bond perpendicular to the molecular plane shown in Figure 4 is extremely small (the TCD magnitudes for 4b in Figure 4 have been scaled by a factor of 5×10^6 compared to the other modes in the figure). Nevertheless, the TCD in this plane reveals cancellation of both translational and circulatory TCDs, as required for the electric dipole and magnetic dipole-forbidden A_u symmetry. Large TCD for this mode (comparable in magnitude to that for the other modes in Figures 4 and 6) is observed in planes perpendicular to the C═C bond and in the plane perpendicular to the molecular plane through the hydrogen nuclei, shown in Figure 7. Projection 1c, through a pair of methylene hydrogen nuclei, exhibits elliptical charge circulation encompassing the entire methylene group, with the long axis of the ellipse tilted from the molecular plane toward the direction of nuclear displacement. The TCD circulation at the carbon in the plane perpendicular to the C═C bond (projection 2c) is even larger than at the methylene hydrogens. The TCD in projection 3c, perpendicular to the molecular plane through cis hydrogen nuclei, demonstrates linear nuclear following TCD in the vicinity of the hydrogens and shows the symmetry-required cancellation of current for the two methylene groups.

The effect on the vibrational TCD of a larger basis set was investigated for the out-of-plane B_{2g} wag (mode 2, with a primary contribution from circulatory TCD) and in-plane B_{1u} CH_2 stretch (mode 9, with a primary contribution from nuclear following TCD) of ethylene. The basis set employed [6-311-(2+,2+)G(p,d), 86 basis functions for ethylene compared to 38 basis functions with 6-31g(d)], included extra diffuse basis functions and produced good agreement with experiment for calculations of vertical electronic transition energies in ethylene with CIS and CIS/MP2 methods.[10] The geometry and frequencies were obtained at the MP2/6-31g(d) level. The TCD patterns calculated with the larger basis sets are nearly identical to those presented in Figures 4 and 6, although the computation time increased by a factor of 10 for the larger basis set. As noted above, although the calculated vibrational frequencies and equilibrium geometries differ for the calculations with the two basis sets and also for the DFT calculations, the (normalized)

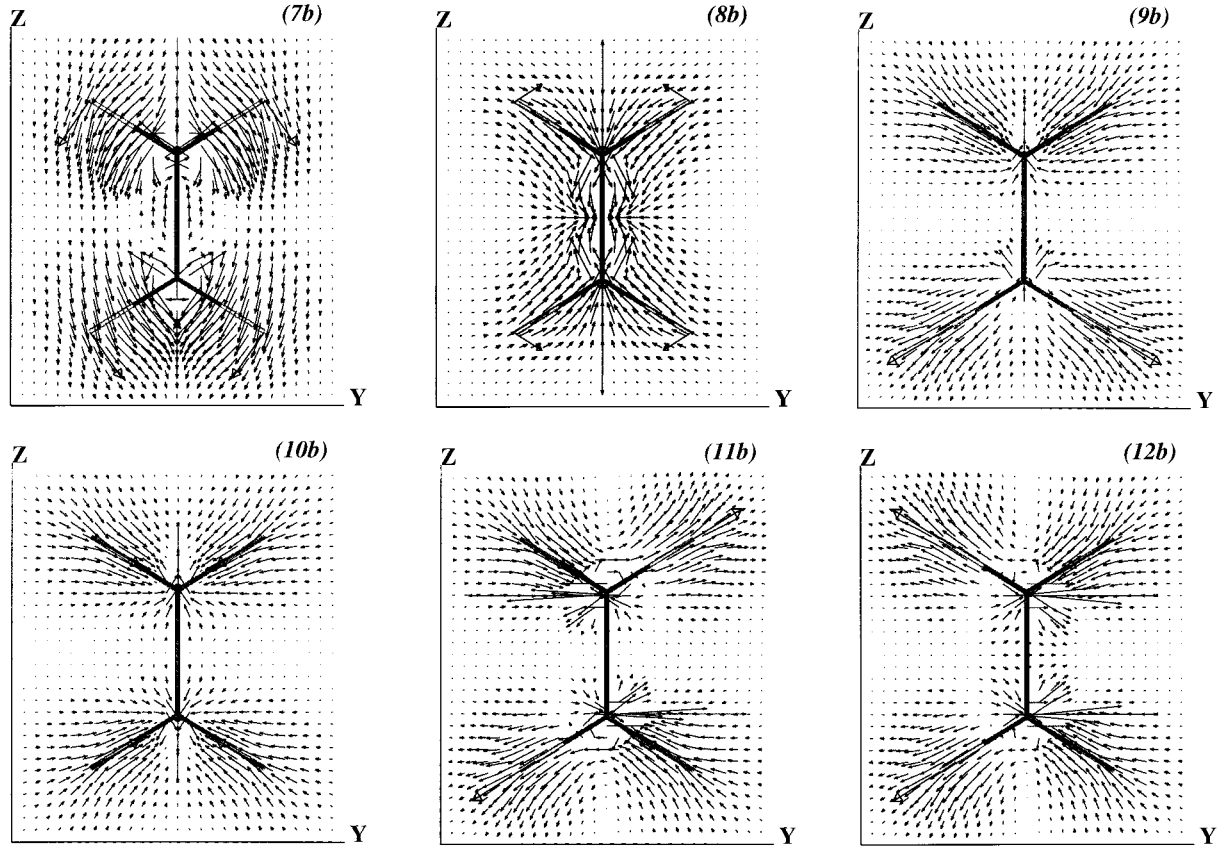

Figure 6. 2D projections of vibrational transition current density (small arrows) and nuclear displacements (large arrows) for the six normal modes of ethylene described in Figure 5, superimposed on wire-frame projections of the molecular structure. Projection plane for the current for these six in-plane modes is the plane of the molecule. TCD vectors have been scaled identically for these six vibrations as for mode 1b.

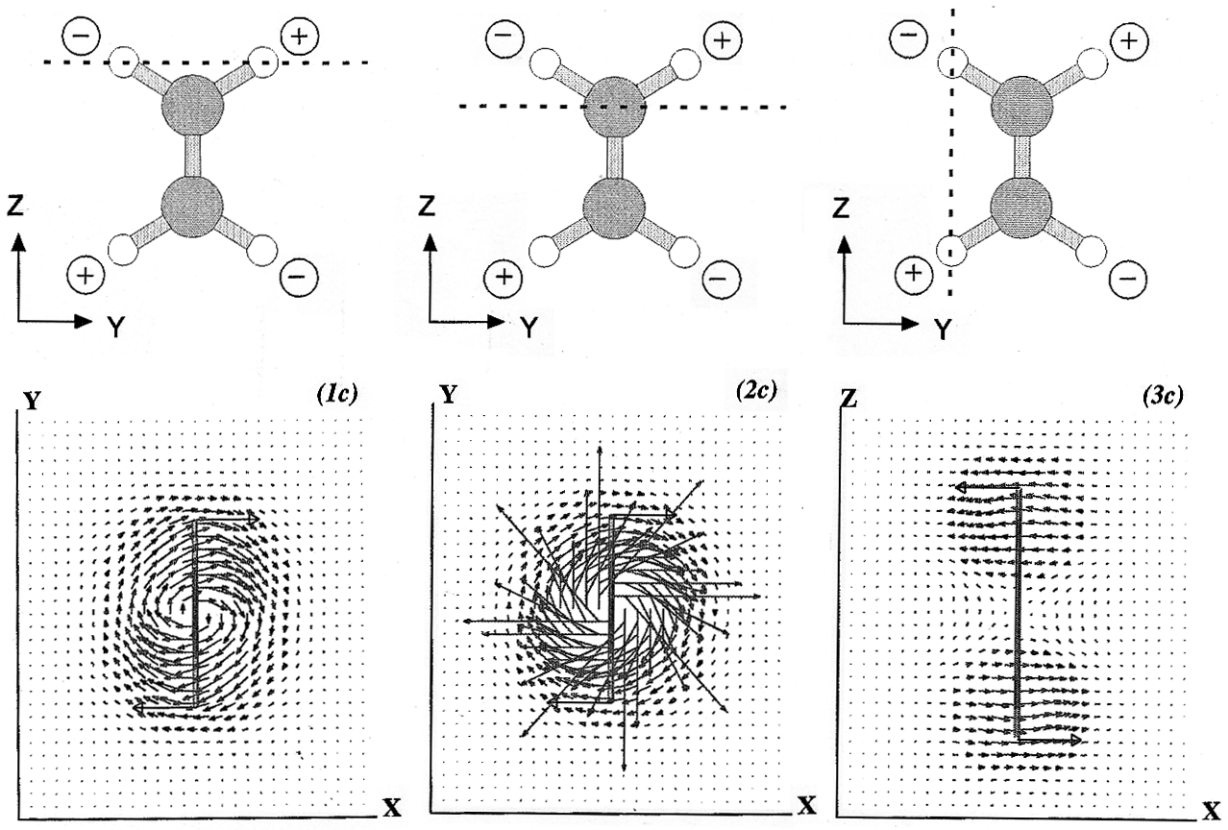

Figure 7. Wire-frame models, nuclear displacements, and vibrational transition current density for the CH_2 twisting mode (4b) of ethylene (lower frames) projected in planes perpendicular to the molecular plane identified by dotted lines in the corresponding upper frames: (1c) through gem hydrogen nuclei; (2c) through carbon center, perpendicular to C═C bond; (3c) through cis hydrogen nuclei. TCD vectors scaled as in Figure 6.

nuclear displacement vectors are identical for this high-symmetry molecule.

Discussion

The vibrational TCD maps display the non-Born−Oppenheimer electron current density resulting from the velocities of the vibrating nuclei. This effect is incorporated into the molecular wave function by means of the complete adiabatic approximation, which introduces the nuclear or vibrational normal mode momenta as classical parameters (these are converted into quantum mechanical operators when operating on the vibrational wave function).[1,3,4] The TCD vector field maps thus depict origin-independent velocity vectors for the electron density at each point in space that accompany the normal mode nuclear velocity vectors shown for each mode. The details of electron flow are lost in presentations of vibrational electron probability difference maps between the electron density in vibrationally displaced and ground nuclear configurations (a scalar field).[11] The vector field $r\Theta^{a}_{g^0,g^1}(r)$ (the integrand of the position-form electric dipole transition moment, defined as transition dipole density) depends on the choice of origin for r, and all vectors would radiate toward or away from that origin and thus do not contain origin-independent charge flow patterns.

Similar to the TCD maps for pure electronic transitions in paper 2 of this series,[2] the vibrational TCD map reveals the symmetry species and dipole selection rules for the vibrational mode. Although the TCD expressions (eqs 1 and 7) involve the linear **p**-operator, and thus directly yield information on the (velocity form) electric dipole transition moment and linear charge flow, visualization of the TCD patterns provides information on higher-order multipole electromagnetic interactions. For example, in addition to the circulatory motion leading to net rotational character and a nonzero magnetic dipole transition moment, as described above, quadrupole character is evident in the ethylene TCD maps for the B_{2g} mode 3b (xz-allowed) and B_{3g} modes 5b and 11b (yz-allowed).

Two types of vibrational TCD are observed for the normal modes of ethylene and formaldehyde, linear or laminar current densities leading to changes in electron probability density, and circulatory current about atomic centers, which contributes only to the magnetic dipole transition moment. The latter effect can be associated with "intrinsic" magnetic dipole transition moment contributions from atomic centers in vibrational circular dichroism.[4,12−15] In addition, angular charge flow across a group of nuclei is evident, for example, for formaldehyde mode 6a or ethylene mode 11b. Such longer range angular charge flow contributes to both the electric and magnetic dipole transition moments and can be descriptively associated with magnetic dipole moment contributions arising from the vector cross products between moment arms from an appropriately located origin to a location of linear charge flow.

The non-Born−Oppenheimer expressions for vibrational TCD require a sum over all excited electronic states. However, we find that the large basis sets required for accurate description

(11) Thieste, D.; Jones, R. D.; Callis, P. R. *Chem. Phys. Lett.* **1987**, *133*, 14.

(12) Nafie, L. A.; Walnut, T. H. *Chem. Phys. Lett.* **1977**, *49*, 441−446.
(13) Nafie, L. A.; Polavarapu, P. L. *J. Chem. Phys.* **1981**, *75*, 2935.
(14) Stephens, P. J. *J. Phys. Chem.* **1987**, *91*, 1712.
(15) Freedman, T. B.; Nafie, L. A.; Yang, D. *Chem. Phys. Lett.* **1994**, *227*, 419−428.

of individual excited states are not required for generating the TCD patterns in these molecules.

Conclusions

These first *ab initio* calculations and maps of vibrational transition current density open a new area for understanding the details of vibrational motion in molecules that considers not only the nuclear motion but also the detailed effects of the nuclear vibration on the electron density of a molecule. Aspects of the motion such as electron current density circulation about an atomic center, which appears to be associated with the lateral motion of adjacent nuclei, are lost when only numerical values of atomic polar and atomic axial tensors are considered in understanding vibrational intensities. In the area of vibrational circular dichroism, where simultaneous linear charge flow and angular charge flow about the direction of the linear flow must occur in order for a vibrational mode of a chiral molecule to exhibit nonzero rotational strength, TCD maps should provide needed new insight into the origin of vibrational circular dichroism intensity. Of particular interest are the origins of the large VCD observed for an isolated oscillator, such as the methine stretch in an α-hydroxy acid, as well as VCD intensity traditionally attributed to local coupled oscillators. Such investigations are currently underway in our laboratory.[16]

Acknowledgment. The authors acknowledge support of this work from the New York State Center for Advanced Technology in Computer Applications and Software Engineering and the W. M. Keck Center for Molecular Electronics, both at Syracuse University, and the National Institutes of Health (GM-23567).

JA9701568

(16) Freedman, T. B.; Gigante, D. M.; Lee, E.; Nafie, L. A, unpublished results.